We are IntechOpen, the world's leading publisher of Open Access books Built by scientists, for scientists

4,800
Open access books available

122,000
International authors and editors

135M
Downloads

Our authors are among the

154
Countries delivered to

TOP 1%
most cited scientists

12.2%
Contributors from top 500 universities

CLARIVATE ANALYTICS BOOK CITATION INDEX INDEXED

WEB OF SCIENCE™

Selection of our books indexed in the Book Citation Index in Web of Science™ Core Collection (BKCI)

Interested in publishing with us?
Contact book.department@intechopen.com

Numbers displayed above are based on latest data collected.
For more information visit www.intechopen.com

6

Quantum Interference Signal from an Inhomogeneously Broadened System Excited by an Optically Phase-Controlled Laser-Pulse Pair

Shin-ichiro Sato and Takayuki Kiba
Division of Biotechnology and Macromolecular Chemistry,
Graduate School of Engineering, Hokkaido University,
Sapporo 060-8628
Japan

1. Introduction

Control of quantum interference (QI) of molecular wavefunctions excited by a pair of femtosecond laser pulses that have a definite optical phase is one of the basic schemes for the control of versatile quantum systems including chemical reactions. The QI technique with the pulse pair, or the double pulse, has been applied to several atomic, molecular systems in gas phase (Scherer et al., 1991; Scherer et al., 1991; Ohmori et al., 2006) and condensed phases (Bonadeo et al., 1998; Mitsumori et al., 1998; Htoon et al., 2002; Sato et al., 2003; Fushitani et al., 2005). A basic theory of the double-pulse QI experiment for a two-level molecular system in gas phase has been given in the original paper by Scherer et al.(Scherer et al., 1991; Scherer et al., 1991). In their beautiful work, they derived the expression for the QI signal from a two-level system including a molecular vibration. However, the effect of inhomogeneous broadening, which is not very significant in the gas phase, has not been taken into account.

Although the overwhelming majority of chemical reactions take place in solution, there have been very few experimental studies on the coherent reaction control of polyatomic molecules in condensed media, due to rapid decoherence of wavefunctions. Electronic dephasing times of polyatomic molecules in solution, which have been mainly measured by photon-echo measurements, are reported to be < 100 fs at room temperature(Fujiwara et al., 1985; Bardeen &Shank, 1993; Nagasawa et al., 2003). These fast quantum-phase relaxations are considered to be caused by solute-solvent interactions such as elastic collisions or inertial (librational) motions (Cho &Fleming, 1993). Thus, understanding the role for the solvent molecules in dephasing mechanism and dynamics is strongly required.

Here, we (1) derive a compact and useful expression for the QI signal for an inhomogeneously broadened two-level system in condensed phases, when the system was excited by an optically phase-controlled laser-pulse pair (Sato, 2007), and (2) introduce our experimental results on the electronic decoherence moderation of perylene molecule in the γ–cyclodextrin (γ-CD) nanocavity (Kiba et al., 2008).

2. Theory

In general, the homogeneous broadening gives a Lorentz profile:

$$S_L(\omega) = \frac{1}{2\pi} \frac{\gamma_l}{(\omega_0 - \omega)^2 + (\gamma_l / 2)^2}. \quad (1)$$

On the other hand, the inhomogeneous broadening gives a Gauss profile:

$$S_G(\omega) = \frac{1}{\sqrt{\pi}\gamma_g} e^{-(\omega-\omega_0)^2/\gamma_g^2}. \quad (2)$$

When both the homogeneous and inhomogeneous broadening exist, the spectral profiles are given by a convolution of $S_L(\omega)$ with $S_G(\omega)$, namely, Voigt profile:

$$S_V(\omega) = \int_{-\infty}^{\infty} d\omega' S_L(\omega') S_G(\omega + \omega_0 - \omega'). \quad (3)$$

As pointed out by Scherer *et al.*, the QI signal is the free-induction decay and the Fourier transform of the optical spectral profile. According to the convolution theorem in the Fourier transform, the expression for the QI signal should have the form in principle:

$$QI(t_d) = FT\left[S_V(\omega)\right] = FT\left[S_L(\omega)\right] \cdot FT\left[S_G(\omega)\right] \propto \cos[\omega_0 t_d] \exp\left[-\frac{\gamma_l t_d}{2}\right] \exp\left[-\frac{\gamma_g^2 t_d^2}{4}\right], \quad (4)$$

where t_d is a time delay between the laser-pulse pair. However, in the above discussion, the laser pulse is assumed to be impulsive, that is, the effects of a finite time width or a spectral width of the actual laser pulse is not taken into accounts. The purpose of this paper is to derive the expression for the QI signal that includes the effects of non-impulsive laser pulses. The procedure for derivation is two steps; first, we derive the expression for the homogeneously broadened two-level system, and then we obtain the expression for the inhomogeneously broadened system by integrating the result of the homogeneously broadened system weighted by the inhomogeneous spectral distribution function.

2.1 homogeneously broadened two-level system

Let us consider a two-level electronic system interacting with a phase-controlled femtosecond-laser pulse pair (Figure 1). When the ground-state energy is assumed to be zero, that is the system is referenced to the molecular frame, the electronic Hamiltonian for the two-level system with the homogeneous broadening is given by

$$\hat{H} = (\varepsilon - i\gamma_l / 2) |e\rangle\langle e|, \quad (5)$$

where γ_l is a homogeneous relaxation constant that stands for a radiative or a non-radiative decay constant. An electronic transition dipole operator is expressed as

$$\hat{\mu} = \mu_{eg} \left(|e\rangle\langle g| + |g\rangle\langle e|\right). \quad (6)$$

The interaction Hamiltonian between the system and a photon field is given by

$$\hat{V} = -\hat{\mu}\, E(t)\,, \tag{7}$$

where photoelectric field $E(t)$ in the double-pulse QI experiments is given by the sum of E_1 and E_2, each of which has a Gauss profile：

$$E(t) = E_1(t) + E_2(t)\,, \tag{8}$$

$$E_1(t) = E_0 \exp\left[-t^2 / 2\tau^2\right]\cos(\Omega t)\,, \tag{9}$$

$$E_2(t) = E_0 \exp\left[-(t-t_d)^2 / 2\tau^2\right]\cos\left[\Omega(t-t_d)\right], \tag{10}$$

where τ is a standard deviation of an each laser pulse in time domain, and related to a standard deviation Γ of the each laser pulse in frequency domain by $\tau = 1/\Gamma$, and Ω is a common carrier frequency of the laser pulses. The phase shift of the photon field is defined as delay-time (Xu et al., 1996): the delay-time t_d between double pulses is finely controlled with attoseconds order in the optical phase-controlled experiments. This definition is natural in the optical phase-shift experiments (Albrecht et al., 1999).
To derive the expression for the QI signal, we divide the time region into the free-evolution regions and the interaction regions. (Fig. 2) Then, the time evolution of the system from the initial electronic state $|\psi(t=0)\rangle = |g\rangle$ is given by the equation:

$$|\psi(t)\rangle = \hat{U}(t - t_d - \delta)\,\hat{W}_2\,\hat{U}(t_d - 2\delta)\,\hat{W}_1\,|g\rangle\,, \tag{11}$$

where the time evolution operator in the absence of the photon field is defined by

$$\hat{U}(t,t') = \exp\left[-i\hat{H}(t-t')/\hbar\right], \tag{12a}$$

or by replacing as $\Delta t = t - t'$

$$\hat{U}(\Delta t) = \exp\left[-i\hat{H}\Delta t/\hbar\right]. \tag{12b}$$

Within the framework of the first order perturbation theory, (Louisell, 1973) the time evolution operator $\hat{W}_j\ (j=1,2)$ in the presence of the photon field is given by

$$\begin{aligned}\hat{W}_j &= \hat{U}(t_j+\delta, t_j-\delta)\left\{1 - \frac{1}{i\hbar}\int_{t_j-\delta}^{t_j+\delta} dt'\,\hat{U}\left(t_j - t'\right)\hat{\mu}\,E_j(t')\,\hat{U}\left(t' - t_j\right)\right\} \\ &= \hat{U}(2\delta)\left\{1 - \frac{1}{i\hbar}\int_{t_j-\delta}^{t_j+\delta} dt'\,\hat{U}\left(t_j - t'\right)\hat{\mu}\,E_j(t')\,\hat{U}\left(t' - t_j\right)\right\} \\ &\equiv \hat{U}(2\delta)\,(1 - \frac{1}{i\hbar}\hat{F}_j)\,.\end{aligned} \tag{13}$$

The substitution of Eq. (9) into Eq. (8) yields

$$|\psi(t)\rangle = \hat{U}(\delta)\left(\hat{U}(t) + \frac{i}{\hbar}\hat{U}(t)\hat{F}_1 + \frac{i}{\hbar}\hat{U}(t-t_d)\,\hat{F}_2\,\hat{U}(t_d)\right)|g\rangle\,, \tag{14}$$

where $\hat{F}$ is defined as an electronic transition operator, and $\hat{U}(\delta)$ a global phase factor, which will be neglected hereafter, because it does not affects final results in the state density matrix. The projection of Eq. (10) onto the excited state $|e\rangle$ gives

$$\begin{aligned}\langle e|\psi(t)\rangle &= \langle e|\left(\hat{U}(t)+\frac{i}{\hbar}\hat{U}(t)\hat{F}_1+\frac{i}{\hbar}\hat{U}(t-t_d)\,\hat{F}_2\,\hat{U}(t_d)\right)|g\rangle \\ &= \frac{i}{\hbar}\langle e|\left(\hat{U}(t)\hat{F}_1+\hat{U}(t-t_d)\,\hat{F}_2\,\hat{U}(t_d)\right)|g\rangle \\ &= \frac{i}{\hbar}\left(\exp\left[(-i\omega_0-\gamma_l/2)\,t\right]\langle e|\hat{F}_1|g\rangle+\exp\left[(-i\omega_0-\gamma_l/2)(t-t_d)\right]\langle e|\hat{F}_2|g\rangle\right)\end{aligned}, \tag{15}$$

where $\omega_0=\varepsilon/\hbar$. The matrix element of an electronic transition operator $\hat{F}_j$ is calculated as

$$\begin{aligned}\langle e|\hat{F}_j|g\rangle &= \langle e|\int_{t_j-\delta}^{t_j+\delta}dt'\,\hat{U}(t_j-t')\,\hat{\mu}\,\hat{U}(t'-t_j)|g\rangle \\ &= \mu_{eg}\langle e|\int_{t_j-\delta}^{t_j+\delta}dt'\,\hat{U}(t_j-t')\left(\,|g\rangle\langle e|+|e\rangle\langle g|\,\right)\hat{U}(t'-t_j)|g\rangle\,E_j(t') \\ &= \mu_{eg}\int_{t_j-\delta}^{t_j+\delta}dt'\,\langle e|U(t_j-t')|e\rangle\langle g|U(t'-t_j)|g\rangle\,E_j(t') \\ &= \mu_{eg}\int_{t_j-\delta}^{t_j+\delta}dt'\,e^{(-i\omega_0-\gamma_l/2)(t_j-t')}E_j(t').\end{aligned} \tag{16}$$

Using a rotating-wave approximation, the matrix element is further calculated as

$$\begin{aligned}\langle e|\hat{F}_j|g\rangle &= \frac{1}{2}E_0\mu_{eg}\int_{-\infty}^{+\infty}dx e^{-i(\omega_0-\Omega)x}e^{-\gamma_l x/2-x^2/(2\tau^2)} \\ &= \sqrt{\frac{\pi}{2}}E_0\mu_{eg}\tau\exp\left[-\frac{(\omega_0-\Omega)^2\tau^2}{2}\right]\equiv F\exp\left[-\frac{(\omega_0-\Omega)^2\tau^2}{2}\right].\end{aligned} \tag{17}$$

The substitution of Eq. (13) into Eq. (11) yields

$$\langle e|\psi(t,t_d)\rangle = \frac{iF}{\hbar}\exp\left[(-i\omega_0-\gamma_l/2)t\right]\left\{\,1+\exp\left[(i\omega_0+\gamma_l/2)\,t_d\,\right]\right\}e^{-(\omega_0-\Omega)^2/(2\Gamma^2)}. \tag{18}$$

The absolute square of Eq. (14) gives the density matrix element $\rho_{ee}(t,t_d,\omega_0,\Omega)$ for the excited state

$$\begin{aligned}\rho_{ee}(t,t_d,\omega_0,\Omega) &= \langle e|\psi(t,t_d)\rangle\langle\psi(t,t_d)|e\rangle \\ &= \frac{2F^2}{\hbar^2}e^{-(\omega_0-\Omega)^2/\Gamma^2}\left\{e^{-\gamma_l t}+e^{-\gamma_l(t-t_d)}+e^{-\gamma_l t/2}e^{-\gamma_l(t-t_d)/2}\cos\left[\omega_0 t_d\right]\right\}.\end{aligned} \tag{19}$$

The first and second term give population decays of the excited state created by the first and second pulses, respectively. The third term is the interference term that is the product of coherence decays and an oscillating term.

2.2 inhomogeneously broadened system

In the previous section, the inhomogeneous broadening was not taken into consideration. The effects of inhomogeneous decay can be taken into account by summing up ρ_{ee} that

originates from inhomogeneously broadened spectral components (Allen &Eberly, 1975). When the inhomogeneous spectrum function is given by a Gauss function in Eq. (2), the expectation value of the excited-state density function can be written as:

$$\begin{aligned}\left\langle \rho_{ee}\left(t_d,\omega_0,\Omega\right)\right\rangle &= \int_{-\infty}^{+\infty} d\omega\, S_{\mathrm{G}}\left(\omega,\omega_0\right)\rho_{ee}\left(t_d,\omega,\Omega\right) \\ &= \frac{F^2}{\hbar^2}\int_{-\infty}^{+\infty} d\omega\, S_{\mathrm{G}}\left(\omega,\omega_0\right)e^{-(\omega-\Omega)^2/\Gamma^2}\left\{e^{-\gamma_l t}+e^{-\gamma_l(t-t_d)}+e^{-\gamma_l t/2}e^{-\gamma_l(t-t_d)/2}\cos\left(\omega\, t_d\right)\right\}\end{aligned} \tag{20}$$

In the above equation, the two-center Gaussian functions can be rewritten as a one-center Gaussian function;

$$\begin{aligned}S_{\mathrm{G}}\left(\omega,\omega_0\right)e^{-(\omega-\Omega)^2/\Gamma^2} &= \frac{1}{\sqrt{\pi}\gamma_g}e^{-(\omega-\omega_0)^2/\gamma_g{}^2}e^{-(\omega-\Omega)^2/\Gamma^2} \\ &= \frac{1}{\sqrt{\pi}\gamma_g}\exp\left[-\frac{\left(\omega_0-\Omega\right)^2}{\gamma_g^2+\Gamma^2}\right]\exp\left[-\frac{\gamma_g^2+\Gamma^2}{\gamma_g^2\,\Gamma^2}\left(\omega-\frac{\Gamma^2\omega_0+\gamma_g^2\,\Omega}{\gamma_g^2+\Gamma^2}\right)^2\right].\end{aligned} \tag{21}$$

By defining a reduced decay constant γ_a and a reduced frequency ω_a;

$$\frac{1}{\gamma_a^2}\equiv\frac{\gamma_g^2+\Gamma^2}{\gamma_g^2\,\Gamma^2}\quad,\quad \omega_a\equiv\frac{\Gamma^2\omega_0+\gamma_g^2\,\Omega}{\gamma_g^2+\Gamma^2} \tag{22}$$

Eq. (21) becomes a simple form:

$$S_{\mathrm{G}}\left(\omega,\omega_0\right)e^{-(\omega-\Omega)^2/\Gamma^2}=\frac{1}{\sqrt{\pi}\gamma_g}\exp\left[-\frac{\left(\omega_0-\Omega\right)^2}{\gamma_g^2+\Gamma^2}\right]\exp\left[-\frac{\left(\omega-\omega_a\right)^2}{\gamma_a^2}\right] \tag{23}$$

By carrying out the Gauss integral and the Fourier integral of the Gaussian function, the final form of Eq. (20) becomes:

$$\left\langle \rho_{ee}\left(t,t_d,\omega_0,\Omega\right)\right\rangle=\frac{\gamma_a}{\gamma_g}\frac{F^2}{\hbar^2}\exp\left[-\frac{\left(\omega_0-\Omega\right)^2}{\gamma_g^2+\Gamma^2}\right]\left\{e^{-\gamma_l t}+e^{-\gamma_l(t-t_d)}+2\cos\left[\omega_a t_d\right]e^{-\gamma_l t/2}e^{-\gamma_l(t-t_d)/2}e^{-\frac{\gamma_a^2 t_d^2}{4}}\right\} \tag{24}$$

In the conventional QI experiments, the QI signal is obtained as total fluorescence integrated over time. Thus, the QI signal is calculated from Eq. (24) as following:

$$\begin{aligned}QI\left(t_d\right) &= -\int_{t_d}^{\infty} dt\frac{d\left\langle \rho_{ee}(t,t_d,\omega_0,\Omega\right\rangle}{dt}dt=\left\langle \rho_{ee}\left(t=t_d,t_d,\omega_0,\Omega\right)\right\rangle \\ &= \frac{\gamma_a}{\gamma_g}\frac{F^2}{\hbar^2}\exp\left[-\frac{\left(\omega_0-\Omega\right)^2}{\gamma_g^2+\Gamma^2}\right]\left\{1+e^{-\gamma_l\, t_d}+2\cos\left[\omega_a t_d\right]e^{\frac{-\gamma_l\, t_d}{2}}e^{-\frac{\gamma_a^2 t_d^2}{4}}\right\}\end{aligned} \tag{25}$$

In the above derivation, the pure dephasing was not taken into account and a transverse relaxation time constant T_2 and a longitudinal relaxation constant T_1 is related by

$$\frac{1}{T_2}=\frac{\gamma_l}{2}=\frac{1}{2T_1}\,. \tag{26}$$

However, in general, there also exists a pure dephasing γ* that is brought about from elastic solute-solvent collisions. (Louisell, 1973) Thus, the transverse relaxation time constant should be rewritten as:

$$\frac{1}{T_2} = \frac{\gamma_l}{2} + \gamma^* = \frac{1}{2T_1} + \frac{1}{T_2^*}$$

The final expression for the QI signal is given by

$$QI(t_d) = \frac{\gamma_a}{\gamma_g}\frac{F^2}{\hbar^2}\exp\left[-\frac{(\omega_0-\Omega)^2}{\gamma_g^2+\Gamma^2}\right]\left\{1+e^{-\frac{t_d}{T_1}}+2\cos[\omega_a t_d]e^{-\frac{t_d}{T_2}}e^{-\frac{\gamma_a^2 t_d^2}{4}}\right\}. \quad (27)$$

By comparing the third term in Eq. (27) with Eq. (4), we obtain

$$QI(t_d) \propto \cos[\omega_a t_d]\exp\left(-\frac{t_d}{T_2}\right)\exp\left(-\frac{\gamma_a^2 t_d^2}{4}\right). \quad (28)$$

We notice that ω_0 and γ_g in the impulsive excitation are replaced by ω_a and γ_a, respectively, in the non-impulsive excitation. These reduced constants, of course, approaches ω_0 and γ_g in the limiting case of impulsive laser pulses; that is, when $\Gamma >> \gamma_g$, the following relations can be deduced.

$$\omega_a \cong \omega_0 \,,\ \gamma_a \cong \gamma_g \,.$$

In the reverse limiting case of $\gamma_g >> \Gamma$, that is, in the case of quasi continuum wave (CW) laser, we notice that

$$\omega_a \cong \Omega \,,\ \gamma_a \cong \Gamma \,.$$

Under this condition, if we further assume that $\frac{1}{T_2} >> \Gamma$, the QI signal can be approximately written as

$$QI(t_d) = \frac{\Gamma}{\gamma_g}\frac{F^2}{\hbar^2}\exp\left[-\frac{(\omega_0-\Omega)^2}{\gamma_g^2}\right]\left\{1+e^{-\frac{t_d}{T_1}}+2\cos[\Omega t_d]e^{-\frac{t_d}{T_2}}\right\}. \quad (28)$$

This result may be the time-domain expression for the hole-burning experiments. These two extreme situations are schematically drawn in Fig. 3. Figure 3 infers that the overlap of the laser-pulse spectrum with the absorption spectrum plays a role of the effective spectral width for the system excited by the non-impulsive laser pulse.

Figure 4 shows the interference term of QI signals calculated for intermediate cases. The red sinusoidal curve of the QI signal was calculated for $\gamma_g = 100\,cm^{-1}$ and $\Gamma = 200\,cm^{-1}$, while the blue one was calculated for $\gamma_g = 200\,cm^{-1}$ and $\Gamma = 100\,cm^{-1}$. All the other parameters were common for the two calculations. The frequency of the QI signal is altered by the ratio of γ_g to Γ for the cases of non-zero detuning (e.g $\omega_0 - \Omega \neq 0$) .

3. Cyclodextrin nanocavity caging effect on electronic dephasing of perylene in γ-CD

It is obvious that the inhibition or the moderation of dephasing is quite important subject for the development of coherent control techniques for more general reactions. In another word, protection of molecular wavefunctions from the surrounding environment becomes important issue for realization of quantum control techniques in condensed phases. For that purpose, we aimed for the protection of the quantum phase of a guest molecule using the size-fit nano-space in a cyclodextrin nanocavity (Kiba et al., 2008).

Cyclodextrins (α-, β-, or γ-CD), which are oligosaccharides with the hydrophobic interior and the hydrophilic exterior, are used as nanocavities because of their unique structures and the fact that six(α-), seven(β-), or eight(γ-) D-glucopyranose units determine the sizes whose diameters are ~5.7, 8.5, and 9.5 Å, respectively. The ability of CDs to encapsulate organic and inorganic molecules in aqueous solution has led to intensive studies of their inclusion complexes.(Douhal, 2004) We intuitively imagined that the confinement of a guest molecule within the CD nanocavity will reduce perturbations from the surrounding environment which causes decoherence. Several studies on CD complexes with aromatic compounds using steady-state and ultrafast time-resolved spectroscopy have been reported (Hamai, 1991; Vajda et al., 1995; Chachisvilis et al., 1998; Matsushita et al., 2004; Pistolis &Malliaris, 2004; Sato et al., 2006). However, there were no experiments, to our knowledge, which interrogate the effect of CD inclusion on the inhibition of decoherence.

3.1 Sample preparation

Perylene (Sigma Chemical Co.), γ-CD (Kanto Kagaku), and tetrahydrofuran (JUNSEI) was used without further purification. A Milli-Q water purification system (Millipore) was used for purification of water. Perylene / γ-CD aqueous solution for measurements was prepared by the following procedure; perylene was deposited by evaporation from saturated ethanol solution into an inner surface of a beaker, and then 10^{-2} M aqueous solution of γ-CD was added into that. The stock solution was sonicated for 5 minutes and stirred 12 hours, and then filtered in order to remove the aggregates of unsolubilized perylene. The concentration of perylene was 5×10^{-7} M that was determined from the absorption spectrum. Steady-state fluorescence and fluorescence-excitation spectra were measured with an F-4500 fluorescence spectrometer (Hitachi) at room temperature.

3.2 Quantum interference measurement using an optical-phase-controlled pulse pair

Experimental setup for the QI measurement is schematically drawn in Figure 5. The optical-phase-controlled pulse pair was generated by splitting femtosecond pulses (844 nm, ~ 40 fs, 80 MHz) from a Ti: sapphire laser (Tsunami, Spectra physics) into two equal parts by means of a Michelson interferometer.(Sato et al., 2003) A delay time t_d of pulse pair was determined by the difference in an optical path length of the two arms of the interferometer. A coarse delay was varied by a stepper-motor-driven mechanical stage on the one arm. A relative optical phase angle of two pulses was controlled with a fine delay produced by a liquid-crystal modulator (LCM, SLM-256, CRI), which can vary an optical delay with tens of atto seconds precision (approximately λ/100 of the laser wavelength). A dual-frequency (f_1 and f_2) mechanical chopper was used to modulate the laser field. The cross-beam fluorescence component that was proportional to E_1E_2 was picked up through lock-in amplifier (NF5610B) referenced to the differential frequency f_1 - f_2. A group velocity dispersion (GVD)

of the laser output from the interferometer was compensated by a prism pair. The pulse pair from the interferometer was frequency-doubled by a BBO crystal. The frequency-doubled pulse pair was reflected by a dichroic mirror (DM) and used to excite a sample molecule, while the fundamental pulse pair transmitted through the DM was used to measure laser-fringe intensity. The fringe intensity measured here was used to determine the relative optical phase angle of two beams. The fluorescence dispersed by a monochromator (P250, Nikon) was detected by a photomultiplier tube (R106, Hamamatsu). The excitation wavelength in this measurement was fixed at 422 nm to minimize the effects of change in laser pulse shape. Fluorescence was measured at the 0-0 peak that was located at 440 nm for bulk solvent and at 450 nm for γ-CD, respectively. The typical pulse duration was obtained to be 47 fs fwhm at the sample point, assuming a Gaussian pulse. All the spectral measurements were performed using a 10 mm cuvette at room temperature (293 K).

3.3 The spectrum narrowing of steady-state fluorescence and fluorescence-excitation spectra of perylene in γ-CD

Steady-State fluorescence and fluorescence-excitation spectra of perylene in a γ-CD aqueous solution and in THF solution are shown in Figure 6. Each excitation wavelength of the fluorescence spectra was 420 nm for γ-CD and 409 nm for THF, respectively. The excitation spectra were measured by monitoring at 480 nm for γ-CD and 470 nm for bulk solvent, respectively. The stoichiometry of perylene/γ-CD complex was confirmed by measuring a pH dependence of their fluorescence spectra. The fluorescence of perylene disappeared with addition of 0.2 M NaOH to the solution. This is because the deprotonation of a neutral γ-CD molecule gives rise to form an anion in alkaline solution; thus the 1:2 complex will be dissociated owing to electronic repulsion forces between two associating γ-CD molecules which have negatively charged hydroxyl groups. This result is consistent with the behavior of 1:2 complex previously reported (Pistolis &Malliaris, 2004).

Quite interesting point in Figure 6 is that the each band in γ-CD were narrowed in comparison with that in bulk solvent, and the vibrational structure due to the ν_{15} mode (in-plane stretching motion of the center ring between the two naphthalene moieties) became clear in γ-CD. This spectral narrowing of perylene in γ-CD was comparable to that measured in MTHF at 77 K (Figure 7). Because the spectral broadening is generally caused by solute-solvent interactions, the spectral narrowing of the guest in γ-CD at room temperature is likely to be caused by the isolation of the guest from the solvent. If perylene molecules were not encapsulated by γ-CD, the broad vibrational structure like those observed in bulk solvents such as n-hexane or THF, which are shown in Figure 7 for comparison, would be observed due to the direct interaction with water molecules in solution. The fluorescence excitation spectra were fitted to a sum of ν_7 and ν_{15} vibronic bands, each of which has a Voigt lineshape. The contributions of the ν_7 and ν_{15} vibrational modes were taken into account in this fitting. The FWHM of the lowest energy vibronic band ($v' = 0$ for both ν_7 and ν_{15} mode) in several solvents are shown in Table. 1. It is remarkable that the linewidth of the vibronic band of perylene in γ-CD is narrowed even compared to that in a non-polar solvent such as *n*-hexane.

Generally speaking, origins of the spectral narrowing for perylene in γ-CD would be brought about from static and dynamic factors. The spectral width observed for molecules in bulk solvents arises from different local environments (static effect) and/or velocity distribution of solvent molecules colliding with solute molecules (dynamical effect). These

effects lead to a Gaussian distribution of electronic energy gaps, that is, an inhomogeneously broadened (ensemble-averaged) spectrum. The interaction with surrounding environment plays a major role for both homogeneous and inhomogeneous broadenings. We intuitively imagine that the spectral narrowing is originated from the isolation of a guest molecule from the surrounding environment. However, the situation is not so simple, since this phenomenon was not observed for every combination of other host/guest CD complexes. For example, the excitation spectra of perylene/γ-CD and anthracene/β-CD complex were shown in Figure 4 in order to compare the spectral linewidth. The significant spectral narrowing was observed for the case of perylene/γ-CD (Figure 8(a)), whereas almost no narrowing was observed for anthracene/β-CD complex (Figure 8(b)). Since both guest molecules are non-polar, the relative extent (size) of guest molecule relative to the CD cavity sizes was a key factor of the spectral narrowing. In aqueous solution of CD inclusion complex, it is well known that the CD nanocavity contains some solvent water molecules accompanied with the guest molecule.(Douhal, 2004) Therefore, the guest molecules don't suffer from the solvent relaxations that would bring about the spectral broadening. Actually, a Stokes-shift in γ-CD was very small (30 cm^{-1}). As shown in Figure 6a, the 0-0 transition bands of fluorescence and excitation spectra in γ-CD were almost overlapped. This spectral feature indicates that there is no space inside the CD cavity for solvent reorientation between photo absorption and emission. On the other hand, for the case of anthracene / β-CD complex, where the cavity size is larger than the guest molecule, the water molecules are loosely captured in CD cavity, in which the water molecules have the degree of freedom to affect the spectral properties of guest molecule. Therefore, the spectral changes (i.e. narrowing and nearly zero Stoke's Shift) are likely to appear only when the size of guest molecule is just-fitted to the interior size of CD cavity.

There is an issue that whether the size-fit effect within CD cavity contributes to homo- or inhomogeneously to the spectral changes. Generally, the homogeneous broadening gives a Lorentz profile, and the inhomogeneous broadening gives a Gauss profile. In condensed phases, the spectral lineshape contains both homo- and inhomogeneous contributions, and is described by Voigtian which is the convolution of a Lorentzian with a Gaussian as described in the theoretical section. In principle, it is possible to separate a homogeneous component from an inhomogeneous component in the steady-state electronic spectra, by fitting each peak to a Voigt function.(Srajer &Champion, 1991) However, this method includes ambiguity since the deconvolution is necessary, and it is troublesome to determine each parameter uniquely. On the other hand, the QI time profile is the Fourier transform of the steady-state spectrum as previously mentioned. This means the QI time profile is the product of homogeneous dephasing (exponential decay) and inhomogeneous dephasing (Gauss-type decay). Thus, the separation of the two components is much easier in time-domain. In the next section, we discuss the distinction between homogeneous and inhomogeneous broadenings from the result of time-domain QI measurements.

3.4 The QI signals of perylene in γ-CD

The QI signals of perylene (solid line) in γ-CD and in THF solution are shown together with the fringe signals (dotted line) in Figure 9. The intensity of the QI signal was plotted as a function of fine time delay which was defined by the liquid-crystal phase-shifter. The QI signal oscillated with the frequency almost twice that of the fringe, since the fringe signal was measured for the fundamental laser light. A QI signal observed in γ-CD survives at 180

fs, although the signal in THF solution almost diminishes at the same delay time. The QI signal should be enhanced or depreciated according to the phase relation of the molecular wave function, and should oscillate with the period corresponding to the energy interval between electronic ground and excited states while quantum phase of molecular wavefunction created by the first pulse is preserved as shown in Eq.(27). Intramolecular vibrational relaxations and/or solute-solvent interactions disturb the quantum phase of a molecular wavefunction created by the first pulse, and induce decoherence of the wavefunctions. Decoherence reduces the amplitude of QI signal decays as the delay time increases. Therefore, a decay curve of the amplitude of the QI signal represents the electronic dephasing of the sample molecules. It should be noted that the dephasing includes homogeneous and inhomogeneous contributions as described in the previous section. Figure 10 displays the envelope function of QI Signal, in which the absolute square root of the QI signal is plotted as a function of the delay time after t_d = 100 fs. We abandoned the data before t_d = 100 fs because the overlapping of the laser-pulse pair deforms the QI time profile. At a glance, the electronic dephasing of perylene in γ-CD is slower than that in THF solution in Fig. 10.

The envelope of QI signal was fitted to the Eq. (28) in order to estimate the homogeneous dephasing time T_2. The QI signal fitting was carried out together with the fitting of steady-state electronic spectra to Voigt functions, simultaneously, in order to eliminate the ambiguity which arises from estimation of the homogeneous dephasing time and the inhomogeneous linewidth value. In this fitting, we used the following procedures; the initial estimated value of homogeneous and inhomogeneous linewidth were obtained from the rough fitting of vibronic bands to the sum of Voigtian. The QI signal was fitted to the Eq. (28) using obtained inhomogeneous linewidth value (γ_g) in order to estimate the homogeneous dephasing time (T_2). We used the vibronic bandwidth value which was overlapped with laser spectrum. Average value of two vibronic band weighted with an area intensity, (ν_7=1, ν_{15}=0), (ν_7=1, ν_{15}=1), was used in the case of γ-CD aqueous solution, and (ν_7=0, ν_{15}=3), (ν_7=1, ν_{15}=1) was used in the case of THF solution. The QI signal of the pure THF solvent and the 10^{-2} M γ-CD aqueous solution were used as an instrumental response function, and the spectral linewidth value of laser pulse (Γ) was calculated from the pulse duration of the instrumental response function. The steady-state spectrum was fitted again by using T_2 obtained from QI signal fitting, and estimated the inhomogeneous linewidth value. The QI signal fitting was carried out again by using the obtained γ_g. Fitting of steady-state spectra and QI signal was iterated until the fitting parameters T_2 and γ_g were converged, and we found the best parameter set which can reconstruct the steady-state spectra and the time profile consistently. The estimated dephasing time constant (T_2), the homogeneous (γ_l) and inhomogeneous (γ_g) linewidth values obtained from QI signal analysis was summarized in Table 2. From the analysis of dephasing curve, the homogeneous electronic dephasing time (T_2) of perylene in THF and γ-CD nanocavity were estimated to be T_2 = 23 ± 3 fs and T_2 = 42 ± 5 fs, respectively. It was found that the encapsulation of perylene molecule into CD nanocavities brings about the lengthening of T_2.

The same excitation wavelength (422 nm) was used for the QI measurements in γ-CD and in THF, in order to avoid the influence caused by the change in laser pulse shape. The same excitation energy caused the situation that a vibrational excess energy above S_1 origin is different for the two measurements since the absorption spectrum of perylene in CD nanocavities are red-shifted from that in THF solution. The excess energies are approximately 1500 cm^{-1} in the γ-CD and 900 cm^{-1} in THF, respectively. In the photon-echo

studies, it was found that the excitation with large vibrational excess energy accelerates the electronic dephasing in large molecules such as cresyl violet; the acceleration was attributed to intramolecular vibrational relaxations. Therefore, the faster electronic dephasing time would be expected for the measurement of CD inclusion complex if only the difference in excess energy were taken into consideration in our experimental condition. However, our experimental finding was opposite; the dephasing time of perylene in γ-CD was longer than that in THF even with the higher excess energy. Therefore, we can conclude that the CD caging effect brings the lengthening of dephasing time, which overcomes the shortening of the dephasing time due to the increased excess energy. The longer dephasing time should be expected when the excitation laser wavelength is located around 0-0 transition of the absorption spectrum.

4. Conclusion

We have shown that the decays of QI signal obtained by the non-impulsive excitation can be written as the product of exponential decay and Gauss decay, and the Gauss decay constant is given by

$$\frac{1}{\gamma_a^2} \equiv \frac{\gamma_g^2 + \Gamma^2}{\gamma_g^2\,\Gamma^2}\,.$$

We have also shown that the frequency of QI signal is given by

$$\omega_a \equiv \frac{\Gamma^2\omega_0 + \gamma_g^2\,\Omega}{\gamma_g^2 + \Gamma^2}\,.$$

In general, it is often difficult to fit the optical absorption spectrum with Voigt functions in the frequency domain, because the Voigt function includes the convolution integral, and one often finds several parameter sets of the least-squared fits. This situation makes it difficult to separate homogeneous components from inhomogeneous components in the frequency-domain spectrum. In contrast, the fitting procedure is rather easier in the QI experiment, once the expression that includes the effect of laser-pulse width is given. This is because the homogeneous and inhomogeneous components are the simple product in the QI experiment. By analyzing the frequency-domain spectrum and the time-domain QI profile simultaneously (e.g. global fit), the reliable determination of homogeneous and inhomogeneous components of relaxations becomes possible.

	Linewidth[a]	$\nu_{exc\ max}$	$\nu_{fluo\ max}$	Stokes-Shift
γ-CD / water	278 cm^{-1}	22245 cm^{-1}	22215 cm^{-1}	30 cm^{-1}
THF	373 cm^{-1}	22837 cm^{-1}	22717 cm^{-1}	120 cm^{-1}
n-hexane	314 cm^{-1}	22959 cm^{-1}	22894 cm^{-1}	65 cm^{-1}

Table 1. Comparison of the electronic spectra of perylene in solutions at room temperature.

a. FWHM of lowest energy vibronic band (v′ = 0 for both ν_7 and ν_{15} mode) resolved from the fluorescence excitation spectra.

	T_2	□g
γ-CD / water	42 ± 5 fs	180 ± 20 cm^{-1}
THF	23 ± 3 fs	270 ± 35 cm^{-1}

Table 2. Best-fit parameter set (homogeneous dephasing time and inhomogeneous linewidth value (FWHM)) obtained from QI signal and steady-state spectra.

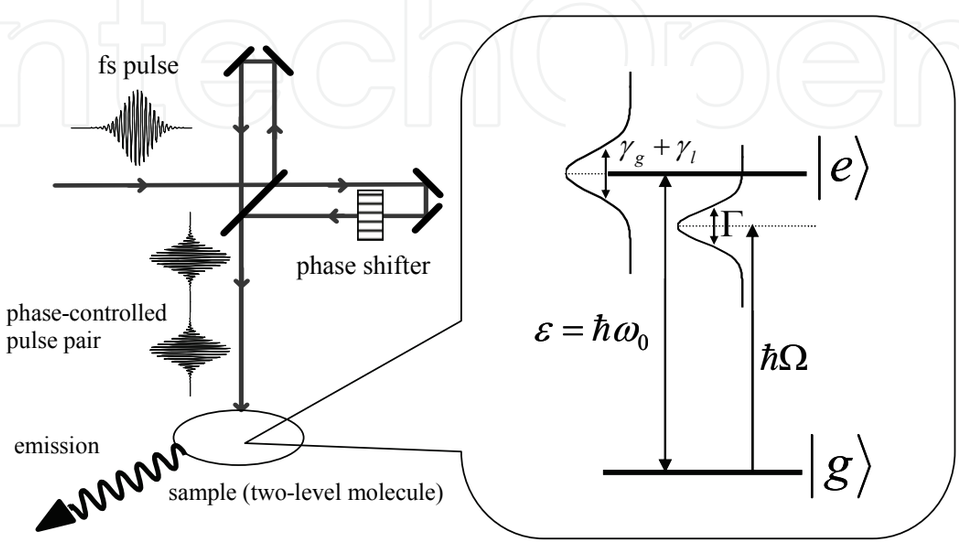

Fig. 1. Schematic drawing of the QI experiment with a phase-controlled laser-pulse pair.

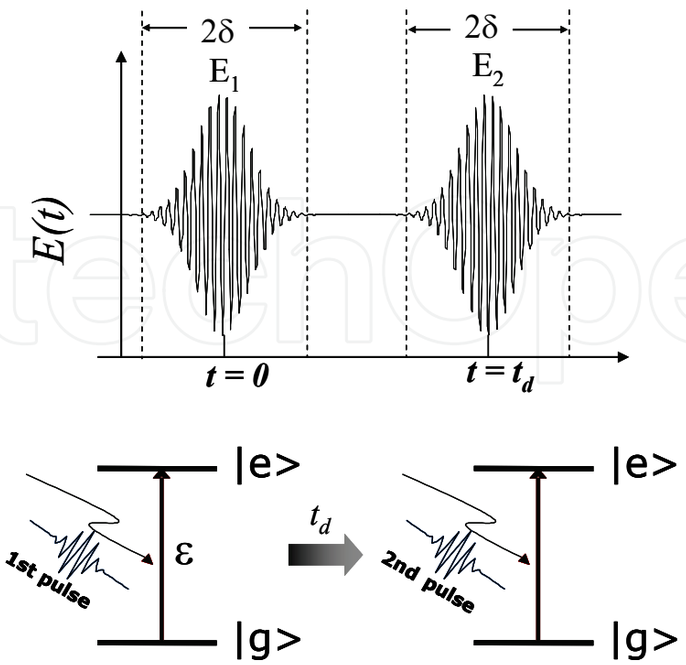

Fig. 2. Time domains: free evolution and interaction with laser pulses.

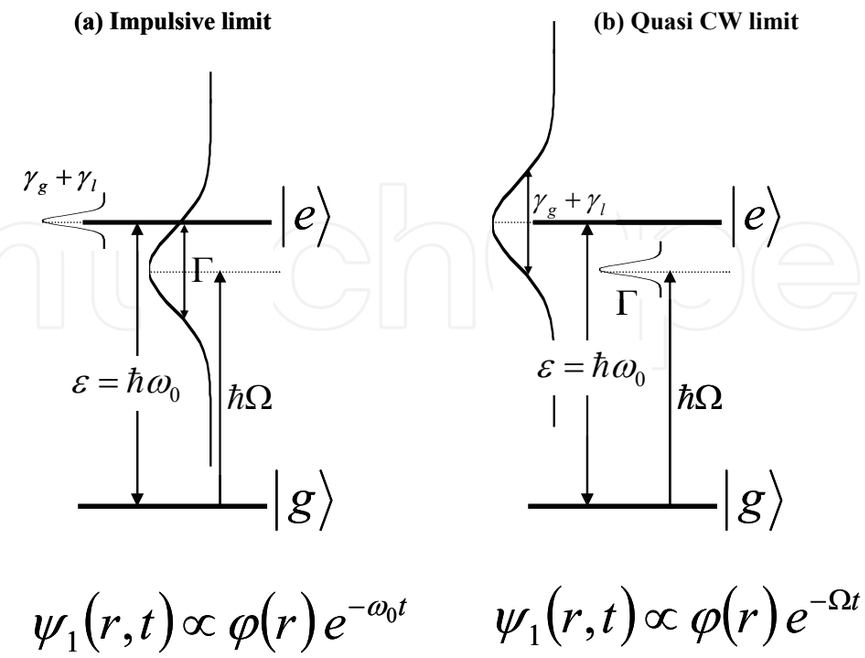

Fig. 3. Limiting cases: impulsive laser (left) and quasi CW laser (right).

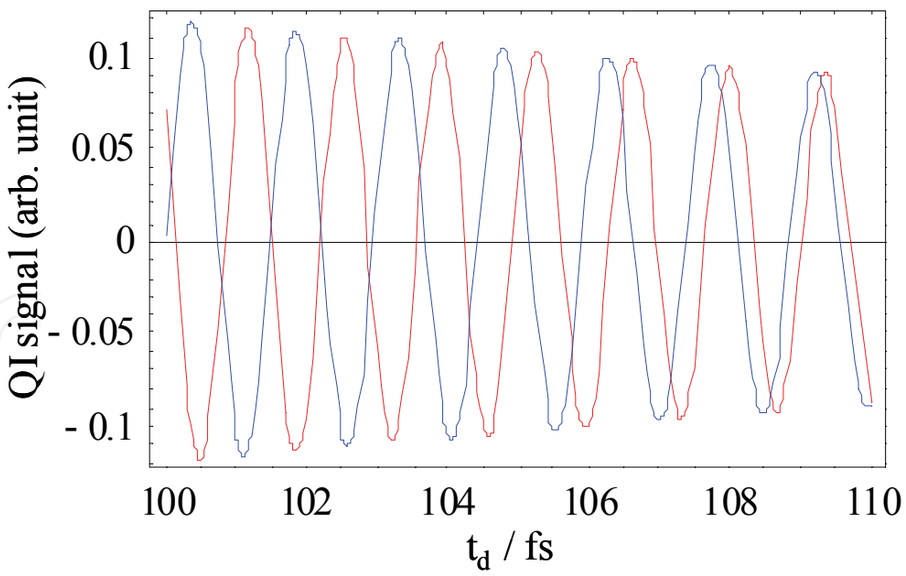

Fig. 4. QI signals simulated for the intermediate cases. The parameters specific for each curve were: $\gamma_g = 100\ cm^{-1}$ and $\Gamma = 200\ cm^{-1}$ (for the red curve), $\gamma_g = 200\ cm^{-1}$ and $\Gamma = 100\ cm^{-1}$ (for the blue curve). The common parameters for the two curves were $\omega_0 = 25000\ cm^{-1}$, $\Omega = 22000\ cm^{-1}$, $\gamma_l = 100 cm^{-1}$, and $\gamma^* = 25\ cm^{-1}$.

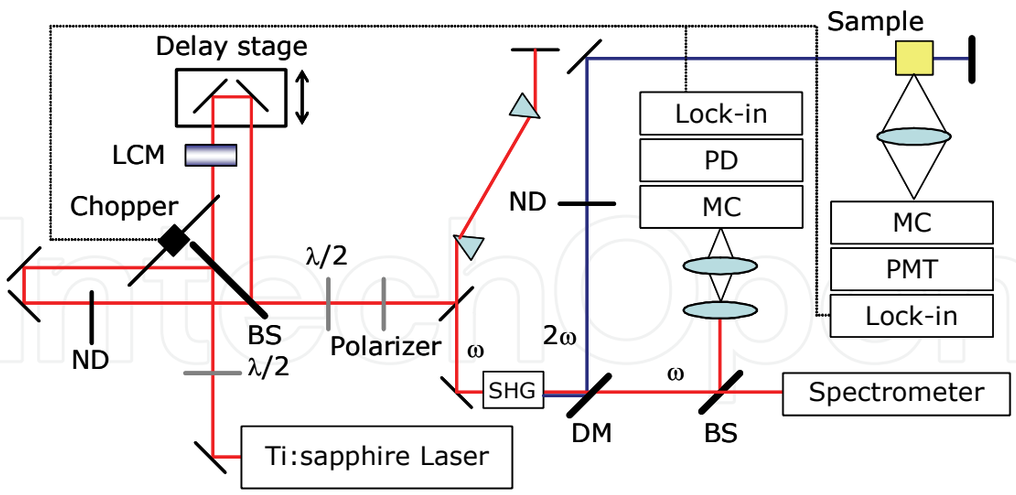

Fig. 5. The experimental setup for the quantum wavepacket interferometry. Abbreviations in the schematic diagram are used for optical beam splitter (BS), the second harmonic generator (SHG), the dichroic mirror (DM), the liquid crystal modulator (LCM), the neutral density filter (ND), monochromator (MC), the photomultiplier (PMT), and the photo diode (PD).

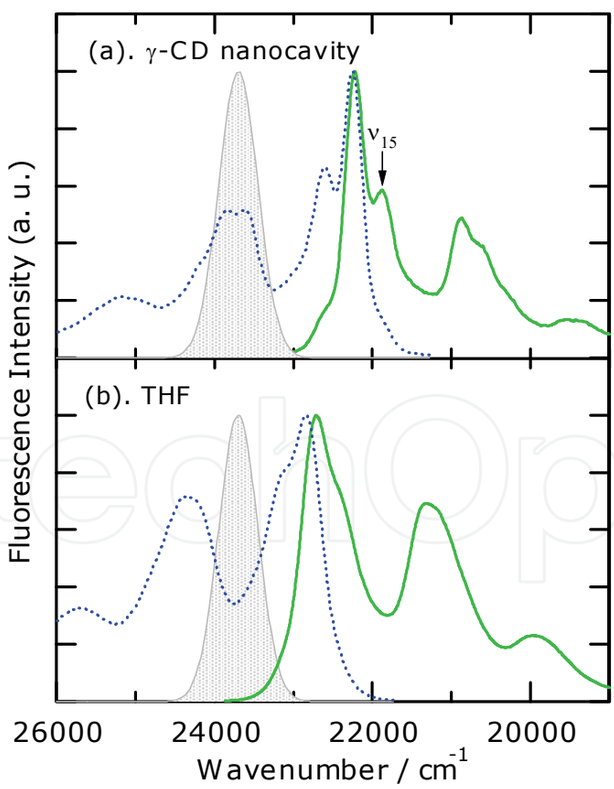

Fig. 6. Steady-state fluorescence (solid line) and fluorescence-excitation (dotted line) spectra of perylene (a) in γ-CD nanocavity and (b) in THF. Spectrum of the excitation pulse used in the quantum interference measurement is also shown for comparison (shaded area).

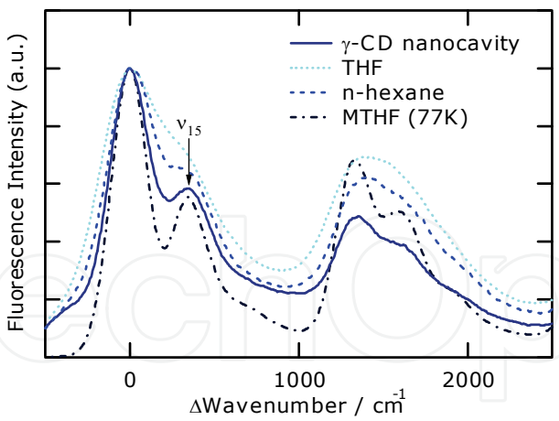

Fig. 7. Steady-state fluorescence spectra of perylene in γ-CD nanocavity (solid line), in THF (dotted line), in n-hexane (dashed line) and in MTHF at 77 K (dash-and-dotted line). The spectra are displayed as wavenumber shift from 0-0 transition in order to compare the spectral line-shapes.

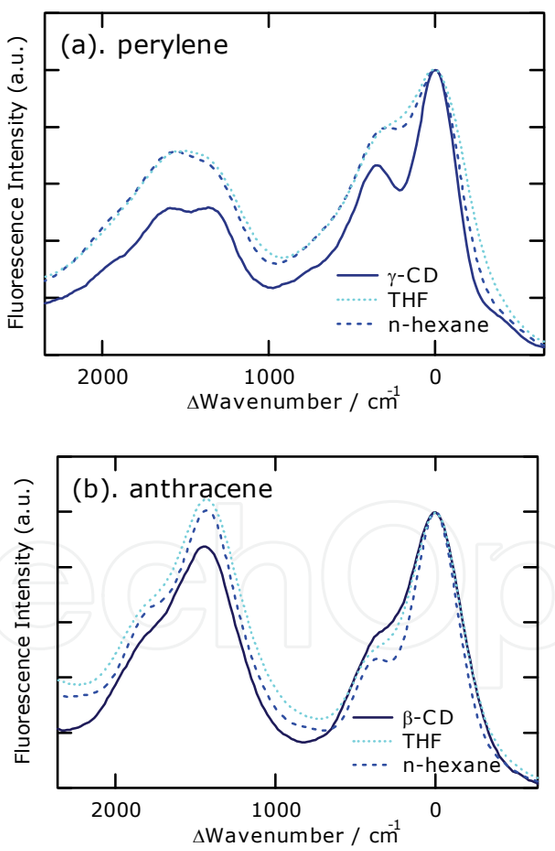

Fig. 8. Steady-state fluorescence-excitation spectra of (a) perylene in γ-CD (solid line), in THF (dotted line) and in n-hexane (dashed line), and (b) anthracene in β-CD (solid line), in THF (dotted line) and in n-hexane (dashed line). The spectra are displayed as wavenumber shift from 0-0 transition in order to compare the spectral line-shapes.

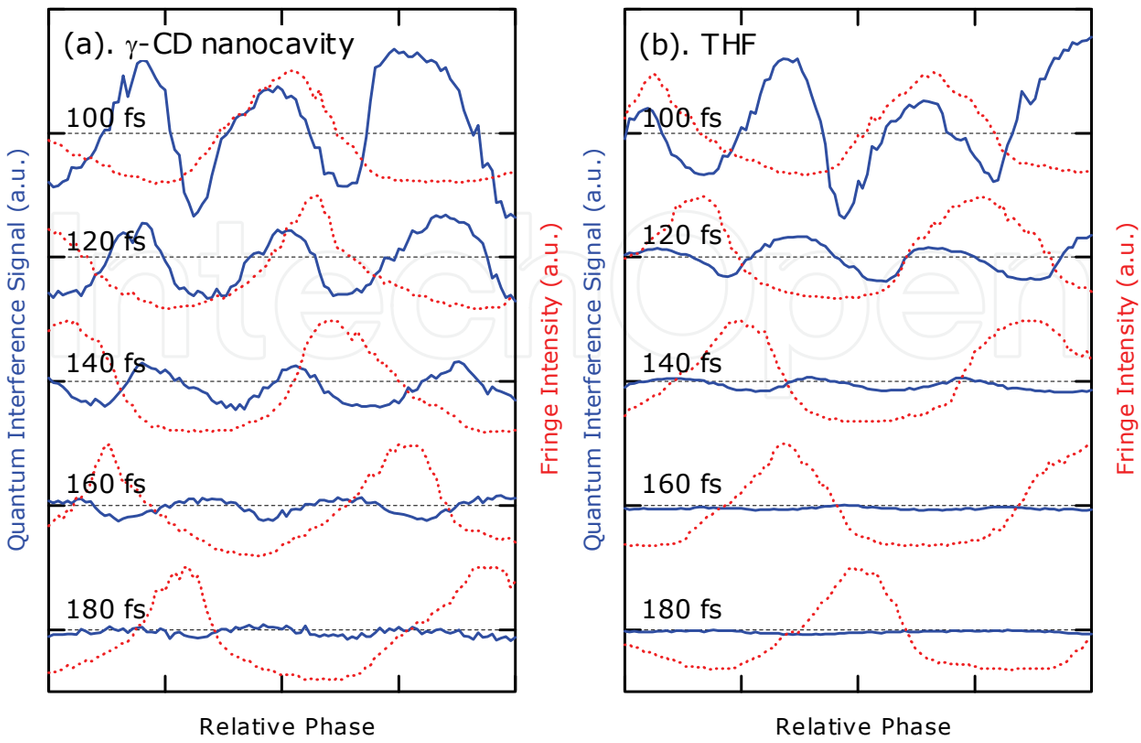

Fig. 9. Quantum interference signals (solid line) of perylene in (a) γ-CD nanocavity and in (b) THF. Fringe signals (dashed line) are also shown as a measure of relative optical phase.

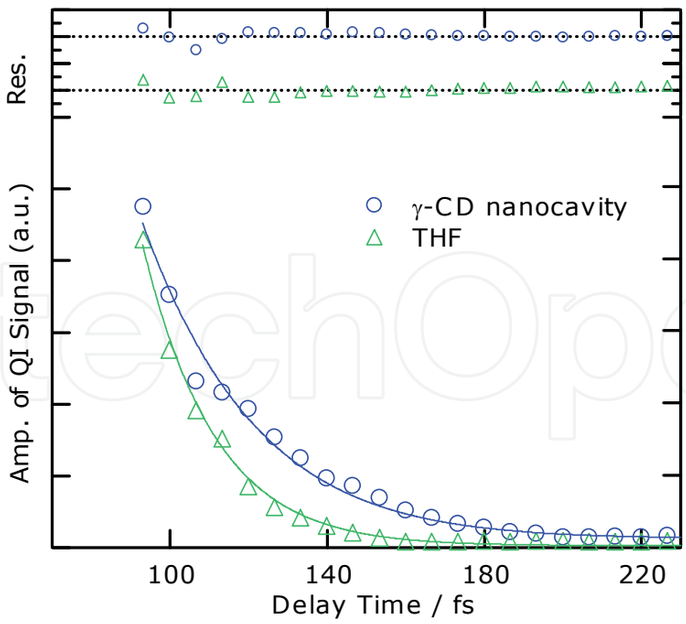

Fig. 10. Electronic dephasing curves of perylene in γ-CD nanocavity (open circles) and in THF (open triangles), where the oscillating amplitude of the QI signal is plotted as a function of the delay time. The dephasing curves were fitted to a theoretical equation. Solid lines are fits of experimental data.

5. References

Albrecht, A. W., Hybl, J. D., Faeder, S. M. G. and Jonas, D. M. (1999). Experimental distinction between phase shifts and time delays: Implications for femtosecond spectroscopy and coherent control of chemical reactions, *Journal of Chemical Physics*, Vol.111, 10934-10956.

Allen, L. and Eberly, J. H. (1975). Optical Resonance and Two-Level Atoms. New York, Dover.

Bardeen, C. J. and Shank, C. V. (1993). Femtosecond electronic dephasing in large molecules in solution using mode suppression, *Chemical Physics Letters*, Vol.203(5,6), 535-539.

Bonadeo, N. H., Erland, J., Gammon, D., Park, D., Katzer, D. S. and Steel, D. G. (1998). Coherent Optical Control of the Quantum State of a Single Quantum Dot, *Science*, Vol.282, 1473-1476.

Chachisvilis, M., Garcia-Ochoa, I., Douhal, A. and Zewail, A. H. (1998). Femtochemistry in nanocavities: dissociation, recombination and vibrational cooling of iodine in cyclodextrin *Chemical Physics Letters*, Vol.293(3-4), 153-159.

Cho, M. and Fleming, G. R. (1993). Photon-echo measurements in liquids: numerical calculations with model systems *Journal of Chemical Physics*, Vol.98(4), 2848-2859.

Douhal, A. (2004). Ultrafast Guest Dynamics in Cyclodextrin Nanocavities, *Chemical Review*, Vol.104, 1955-1976.

Fujiwara, M., Kuroda, R. and Nakatsuka, H. (1985). Measurement of ultrafast dephasing time of Cresyl Fast Violet in cellulose by photon echcues with incoherent light, *Journal of Optical Society of America B*, Vol.2, 1634-1639.

Fushitani, M., Bargheer, M., hr, M. G. and Schwentner, N. (2005). Pump–probe spectroscopy with phase-locked pulses in the condensed phase: decoherence and control of vibrational wavepackets, *Physical Chemistry Chemical Physics*, Vol.7, 3143-3149.

Hamai, S. (1991). Exciplex Formaition between Perylene and N,N-Simethylaniline in a Ternary Inclusion Compound with γ-Cyclodextrin in H_2O-Ethanol (7:3) Mixture, *Bulletin of the Chemical Society of Japan*, Vol.64, 431-438.

Htoon, H., Takagahara, T., Kulik, D., Baklenov, O., A. L. Holmes, J. and Shih, C. K. (2002). Interplay of Rabi Oscillations and Quantum Interference in Semiconductor Quantum Dots, *Physical Review Letters*, Vol.88, 087401-1-4.

Kiba, T., Kasajima, T., Nishimura, Y. and Sato, S.-i. (2008). Cyclodextrin Nanocavity Caging Effect on Electronic Dephasing, *ChemPhysChem*(9), 241-244.

Louisell, W. H. (1973). Quantum Statistical Properties of Radiation. New York, John Wiley & Sons, Inc.

Matsushita, Y., Suzuki, T., Ichimura, T. and Hikida, T. (2004). Cavity Size Effect on the Excited State Dynamics of Methyl 4-(Dimethylamino)benzoate-Cyclodextrin Complexes, *Journal of Physical Chemistry A*, Vol.108, 7490-7496.

Mitsumori, Y., Mizuno, M., Tanji, S., Kuroda, T. and Minami, F. (1998). Coherent transients involving 2P excitons in ZnSe, *Journal of Luminescence*, Vol.76&77, 113-115.

Nagasawa, Y., Seike, K., Muromoto, T. and Okada, T. (2003). Two-Dimensional Analysis of Integrated Three-Pulse Photon Echo Signals of Nile Blue Doped in PMMA, *Journal of Physical Chemistry A*, Vol.107(14), 2431-2441.

Ohmori, K., Katsuki, H., Chiba, H., Honda, M., Hagihara, Y., Fujiwara, K., Sato, Y. and Ueda, K. (2006). Real-Time Observation of Phase-Controlled Molecular Wave-Packet Interference, *Physical Review Letters*, Vol.96, 093002.

Pistolis, G. and Malliaris, A. (2004). Evidence for Highly Selective Supramolecular Formation between Perylene/ç-CD and Pyrene/ç-CD Complexes in Water, *Journal of Physical Chemistry B*, Vol.108, 2846-2850.

Sato, S.-i. (2007). Theory of the Quantum Interference Signal from an Inhomogeneously Broadened Two-Level System Excited by an Optically Phase-Controlled Laser-Pulse Pair, *Journal of Chemical Theory and Computation*, Vol.3, 1158-1162.

Sato, S.-i., Nakamura, T., Nitobe, S., Kiba, T., Hosokawa, K., Kasajima, T., Otsuka, I., Akimoto, S. and Kakuchi, T. (2006). Structure and Excitation Relaxation Dynamics of Dimethylanthracene Dimer in a γ-Cyclodextrin Nanocavity in Aqueous Solution, *Journal of Physical Chemistry B*, Vol.110, 21444-21449.

Sato, S.-i., Nishimura, Y., Sakata, Y. and Yamazaki, I. (2003). Coherent Control of Oscillatory Excitation Transfer in Dithia-1,5[3,3]anthracenophane by a Phase-Locked Femtosecond Pulse Pair, *Journal of Physical Chemistry A*, Vol.107, 10019-10025.

Scherer, N. F., Carlson, R. J., Matro, A., Du, M., Ruggiero, A. J., Romero-Rochin, V., Cina, J. A., Fleming, G. R. and Rice, S. A. (1991). Fluorescence-detected wave packet interferometry: Time resolved molecular spectroscopy with sequences of femtosecond phase-locked pulses, *Journal of Chemical Physics*, Vol.95, 1487-1511.

Scherer, N. F., Matro, A., Ziegler, L. D., Du, M., Carlson, R. J., Cina, J. A. and Fleming, G. R. (1991). Fluorescence-detected wave packet interferometry. II. Role of rotations and determination of the susceptibility, *Journal of Chemical Physics*, Vol.96, 4180-4194.

Srajer, V. and Champion, P. M. (1991). Investigations of Optical Line Shapes and Kinetic Hole Burning in Myoglobin, *Biochemistry*, Vol.30, 7390-7402.

Vajda, S., Jimenez, R., Rosenthal, S. J., Fidler, V., Fleming, G. R. and Castner, E. W., Jr. (1995). Femtosecond to nanosecond solvation dynamics in pure water and inside the g-cyclodextrin cavity., *Journal of the Chemical Society, Faraday Transactions*, Vol.91, 867-873.

Xu, L., Spielmann, C., Poppe, A., Brabec, T., Krausz, F. and Hänsch, T. W. (1996). Route to phase control of ultrashort light pulses, *Optics Letters*, Vol.21, 2008-2010.

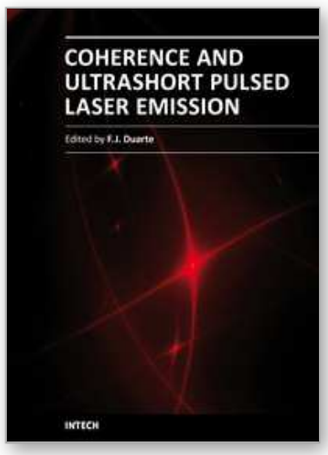

Coherence and Ultrashort Pulse Laser Emission

Edited by Dr. F. J. Duarte

ISBN 978-953-307-242-5
Hard cover, 688 pages
Publisher InTech
Published online 30, November, 2010
Published in print edition November, 2010

In this volume, recent contributions on coherence provide a useful perspective on the diversity of various coherent sources of emission and coherent related phenomena of current interest. These papers provide a preamble for a larger collection of contributions on ultrashort pulse laser generation and ultrashort pulse laser phenomena. Papers on ultrashort pulse phenomena include works on few cycle pulses, high-power generation, propagation in various media, to various applications of current interest. Undoubtedly, Coherence and Ultrashort Pulse Emission offers a rich and practical perspective on this rapidly evolving field.

InTech Europe
University Campus STeP Ri
Slavka Krautzeka 83/A
51000 Rijeka, Croatia
Phone: +385 (51) 770 447
Fax: +385 (51) 686 166
www.intechopen.com

InTech China
Unit 405, Office Block, Hotel Equatorial Shanghai
No.65, Yan An Road (West), Shanghai, 200040, China
中国上海市延安西路65号上海国际贵都大饭店办公楼405单元
Phone: +86-21-62489820
Fax: +86-21-62489821

IntechOpen